

GREY PREDICTION BASED PARTICLE FILTER FOR MANEUVERING TARGET TRACKING

J.-F. Chen, Z.-G. Shi, S.-H. Hong, and K.-S. Chen

Department of Information and Electronic Engineering
Zhejiang University
Hangzhou 310027, China

Abstract—For maneuvering target tracking, we propose a novel grey prediction based particle filter (GP-PF), which incorporates the grey prediction algorithm into the standard particle filter (SPF). The basic idea of the GP-PF is that new particles are sampled by both the state transition prior and the grey prediction algorithm. Since the grey prediction algorithm is a kind of model-free method and is able to predict the system state based on historical measurements other than establishing *a priori* dynamic model, the GP-PF can significantly alleviate the sample degeneracy problem which is common in SPF, especially when it is used for maneuvering target tracking. Simulations are conducted in the context of two typical maneuvering motion scenarios and the results indicate that the overall performance of the proposed GP-PF is better than the SPF and the multiple model particle filter (MMPF) when the tracking accuracy, computational complexity and tracking lost probability are considered. The performance improvements can be attributed to that the GP-PF has both model-based and model-free features.

1. INTRODUCTION

The problem of target tracking has been an important issue of signal processing for many years, and a variety of tracking methods have been proposed in literatures [1–4]. For linear Gaussian problems, the Kalman Filter (KF) can be applied to obtain optimal solutions [5–7]. For nonlinear problems, many nonlinear filtering techniques have been proposed, such as Extended Kalman Filter (EKF) and Unscented Kalman Filter (UKF), which are usually implemented to provide

Corresponding author: Z.-G. Shi (shizg@zju.edu.cn).

Gaussian approximation to the posterior probability density function (pdf) in the state space [8–10]. In recent years, the sequential Monte Carlo methods, also known as particle filters (PFs) [11], have attracted a lot of researchers' attention [12–17]. The key idea of this technique is to represent the probability density by a set of samples with their associated weights. Due to this sample-based representation, particle filters are able to represent a wide range of probability densities, allowing online, real-time estimation of nonlinear, non-Gaussian dynamic systems. Thus, particle filters have been applied with great success to a variety of target tracking problems [18–21].

All the target tracking methods mentioned above are model-based. They assume that the target motion and its observations can be represented by some known mathematical models with sufficient accuracy [22]. However, it is generally difficult to use a single model to represent the motion of a maneuvering target, as the maneuvers are often abruptly deviated from the preceding motion. Hence, multiple model (MM) based approaches are often used for maneuvering target tracking to cover the true dynamics of the target [23, 24]. Though MM-based methods have shown attractive benefits in many situations, these algorithms require as many predetermined sub-models as necessary to handle the varying target maneuver characteristics [25]. This may not only incur extra computational complexity, but also leads to estimation accuracy degradation in cases that some of the models do not match the target motion well. The selection of a proper model set is always a difficult problem [26, 27]. To overcome this problem, the idea of variable structure multiple model and adaptive multiple model methods are proposed [28, 29], where the model set is time-varying and adaptive. Though these methods provide possible ways in some situations, they require much more extra information, such as the target acceleration, the road map, etc., which are hard to obtain in the real-world applications.

To overcome the drawbacks of MM-based algorithms, in this paper, we incorporate the grey prediction [30, 31], which is a model-free method and requires no *a priori* dynamic model of target, into the standard particle filter (SPF) for maneuvering target tracking. The proposed grey prediction based particle filter (GP-PF) has both the inherent advantages of model-based and model-free system, and thus can improve the maneuvering target tracking performance.

The paper is organized as follows: in Section 2, the constant velocity model and the basic concept of grey prediction are described, and the proposed GP-PF algorithm is presented in detail; in Section 3 we compare the tracking performance of the proposed GP-PF, the SPF

and the multiple model particle filter (MMPF) in terms of tracking accuracy, computational complexity and tracking lost probability; in Section 4, conclusion remarks are made.

2. GREY PREDICTION BASED PARTICLE FILTER (GP-PF)

2.1. Constant Velocity Model

The model-based target tracking methods assume that the target motion and its observations are represented by some known mathematic models. One of the most frequently used and simplest target motion model is the constant velocity model [22], which will be used in the proposed GP-PF algorithm. The constant velocity model is generally described as:

$$x_k = A(T)x_{k-1} + B(T)\omega_k \tag{1}$$

where $x_k = [x_k, \dot{x}_k, y_k, \dot{y}_k]'$ is target state vector at time kT (k is the time index and T is the sampling interval); The variables (x_k, y_k) and (\dot{x}_k, \dot{y}_k) represent the target position, speed in the x and y coordinate,

respectively; $A = \begin{pmatrix} 1 & T & 0 & 0 \\ 0 & 1 & 0 & 0 \\ 0 & 0 & 1 & T \\ 0 & 0 & 0 & 1 \end{pmatrix}$ is the state transition matrix, and

$B = \begin{pmatrix} T^2/2 & 0 \\ T & 0 \\ 0 & T^2/2 \\ 0 & T \end{pmatrix}$ is the noise matrix; ω_k is the vector of input

white noise with zero mean and covariance matrix Q .

The measurement equation is

$$z_k = Hx_k + v_k \tag{2}$$

where the measurement matrix H is defined as $H = \begin{pmatrix} 1 & 0 & 0 & 0 \\ 0 & 0 & 1 & 0 \end{pmatrix}$.

It is obvious that $z_k = [z_k^x, z_k^y]'$ consists of position measurements in the x and y direction. The measurement noise v_k is a zero-mean Gaussian noise vector with covariance matrix R .

2.2. Grey Prediction

The grey prediction was firstly introduced in 1982 [32]. It is able to analyze the indeterminate and incomplete data to establish the

systematic relations. It assumes the internal structure, parameters, and characteristics of the observed system are unknown. The system state can be predicted by a differential equation from the recently historical measurements. The grey prediction has been widely used in applications of social sciences, agriculture, procreation, power consumption, and management.

The basic procedure for grey prediction is as follows [33]:

Step 1: Construct a data series that contains the recent measurements:

$$\begin{aligned} z^{(0)} &= \left\{ z^{(0)}(1), z^{(0)}(2), \dots, z^{(0)}(n) \right\} \\ &= \left\{ z^{(0)}(k); k = 1, 2, \dots, n \right\} \end{aligned} \quad (3)$$

where $z^{(0)}(k)$ is the measurement from sensory information at time k and n is the length of the data series.

Step 2: Form a new data series $z^{(1)}$ by an accumulated generating operation (AGO):

$$\begin{aligned} z^{(1)} &= \left\{ z^{(1)}(1), z^{(1)}(2), \dots, z^{(1)}(n) \right\} \\ &= \left\{ z^{(1)}(k); k = 1, 2, \dots, n \right\} \end{aligned} \quad (4)$$

where

$$z^{(1)}(k) = \left\{ \sum_{i=1}^k z^{(0)}(i), k = 1, 2, \dots, n \right\} \quad (5)$$

Step 3: Form the grey differential equation:

$$\frac{dz^{(1)}}{dt} + az^{(1)} = b \quad (6)$$

with initial condition $z^{(1)}(1) = z^{(0)}(1)$. The coefficients, a and b , can be obtained by using the least square method, as shown in (7):

$$\hat{a} = \begin{bmatrix} a \\ b \end{bmatrix} = (B^T B)^{-1} B^T Y_N \quad (7)$$

where $B = \begin{bmatrix} -Z^{(1)}(2) & 1 \\ -Z^{(1)}(3) & 1 \\ \dots & \dots \\ -Z^{(1)}(n) & 1 \end{bmatrix}$, $Y_N = \begin{bmatrix} z^{(0)}(2) \\ z^{(0)}(3) \\ \dots \\ z^{(0)}(n) \end{bmatrix}$, and $Z^{(1)}(k) = \alpha z^{(1)}(k) + (1 - \alpha)z^{(1)}(k - 1), k = 2, 3, \dots, n$, α is the weighting factor.

Step 4: Obtain the prediction value:

Once a and b in (6) are obtained, the grey differential equation can be used to predict the value of state z at time instant $k + 1$.

The AGO grey prediction model can be obtained:

$$\hat{z}^{(1)}(k + 1) = \left[z^{(0)}(1) - \frac{b}{a} \right] e^{-ak} + \frac{b}{a}, \quad k = 0, 1, \dots \tag{8}$$

Then the prediction value of the state can be calculated by an inverse accumulated generating operation (IAGO):

$$\begin{aligned} \hat{z}^{(0)}(k + 1) &= \hat{z}^{(1)}(k + 1) - \hat{z}^{(1)}(k) \\ &= \left(1 - e^{-a} \right) \left[z^{(0)}(1) - \frac{b}{a} \right] e^{-ak} \end{aligned} \tag{9}$$

2.3. Proposed GP-PF

In this section the proposed GP-PF algorithm is presented. For completeness, a brief review of SPF is described first.

Unlike the conventional analytical approximation methods, particle filters are commonly used for the approximation of intractable integrals and rely on the ability to draw random samples (or particles) from a probability distribution. The key idea is to represent the posterior probability density function of the target state given the observations by a set of random particles $\{x_k^j\}_{j=1}^N$ with their associated weights $\{w_k^j\}_{j=1}^N$, where k is the time index, j is the particle index and N is particle number, i.e.,

$$p(x_k | z_k) = \frac{1}{W_k} \sum_{j=1}^N w_k^j \delta(x_k - x_k^j) \tag{10}$$

where $W_k = \sum_{j=1}^N w_k^j$. Then one can compute an optimal estimate based on these particles and weights. In the processing of particle filters, generally there are three important operations [12]:

1) Sampling: generating new particles $x_k^j \sim \pi(x_k | x_{k-1}^j, z_{1:k})$ for $j = 1, \dots, N$, where $\pi(x_k | x_{k-1}^j, z_{1:k})$ is the proposal distribution. The

most popular choice of the proposal distribution is the transition prior $\pi(x_k | x_{k-1}^j, z_k) = p(x_k | x_{k-1}^j)$ due to its simplicity.

2) Weight: assigning an importance weight w_k^j to the particle x_k^j based on the received observations as follows:

$$w_k^j = w_{k-1}^j \frac{p(z_k | x_k^j) p(x_k^j | x_{k-1}^j)}{\pi(x_k^j | x_{k-1}^j, z_{1:k})} \quad (11)$$

followed by normalization $w_k^j = w_k^j \left[\sum_{j=1}^N w_k^j \right]^{-1}$.

3) Resampling: drawing new particles $\{\tilde{x}_k^j\}_{j=1}^N$ from the above set of particles $\{x_k^j\}_{j=1}^N$ based on the particle weights according to a resampling algorithm.

As model-based methods, particle filters are implemented on the base of state model and measurement model. In the SPF, the transition prior is used as the proposal distribution, thus, the sampling operation is conducted according to the target state equation, and the weights are calculated according to the measurement equation. If the models represent the target's dynamics and measurements well, good performance may be obtained by the SPF. However, when maneuvering target tracking problems are considered, the true dynamics is hard to be represented accurately, and this may lead to the sample degeneracy problem [34], where almost all particles have negligible weights after a few iterations. This phenomenon implies that a large amount of computational efforts will be devoted to updating particles whose contribution to the approximation of $p(x_k | z_k)$ is almost zero. This means that the sampled particles contain little information about the true target state and the tracking performance will consequently be degraded.

In order to alleviate this sample degeneracy problem, we try to take advantage of the grey prediction and incorporate it into the particle filter. As described in Section 2.2, the grey prediction is a kind of model-free method, and can predict the trend of system state when some historical measurements are available. Since the grey prediction does not require establishing *a priori* dynamic model of the target, it can compensate those drawbacks of the model-based methods.

The key idea of the GP-PF is that new particles are sampled by two ways: one is by the state transition prior, as in the operation of the SPF, and the other is by the grey prediction. That is, at every time index k , some of the particles are sampled by the state transition prior from particles of time index $k-1$; meanwhile, the other

particles are obtained based on the recent measurements $z_{(k-L):(k-1)}^x$ and $z_{(k-L):(k-1)}^y$ by running the grey prediction algorithm. These two parts of particles form the total particles, and then the weighting, estimating and resampling are followed as the SPF.

Table 1. The outline of the GP-PF algorithm.

<p>Initialization: $k = 0$ for $j = 1, \dots, N_p$ Generate samples $\{x_0^j \sim p(x_0)\}$ Calculate weight $w^j = 1/N_p$ end for $k = 1, 2, \dots$ (main loop) Grey Prediction $X_k^{grey} = \text{grey_prediction}(z_{(k-L):(k-1)}^x), k = L + 1, L + 2, \dots$ $Y_k^{grey} = \text{grey_prediction}(z_{(k-L):(k-1)}^y), k = L + 1, L + 2, \dots$ Sampling Step Grey prediction based sampling for $j = 1 : N_p^{grey}$, generate samples: $x_k^j = \begin{bmatrix} X_k^{grey} \\ vx_k \\ Y_k^{grey} \\ vy_k \end{bmatrix} + B(T)\omega_k^j$ where $vx_k = (X_k^{grey} - X_{k-1}^{grey})/T$, $vy_k = (Y_k^{grey} - Y_{k-1}^{grey})/T$, and $\omega_k^j \sim N(0, Q)$ end Normal sampling for $j = (N_p^{grey} + 1) : N_p$, generate samples: $x_k^j = A(T)x_{k-1}^j + B(T)\omega_k^j$ end Importance Step for $j = 1 : N_p$, calculate the importance weights: $w_k^j = w_{k-1}^j p(z_k x_k^j)$, end followed by normalization: $\bar{w}_k^j = w_k^j / \sum_{j=1}^{N_p} w_k^j$ State Estimation Step $\hat{x} = E[x_k z_{1:k}] = \sum_{j=1}^{N_p} \bar{w}_k^j x_k^j$ Resampling Step end</p>
--

The outline of the GP-PF is shown in Table 1, where $p(x_0)$ is the initial probability for the state vector; N_p is the total number of particles, and N_p^{grey} is the number of particles generated by grey prediction; *grey_prediction* is the function that performs the grey prediction algorithm described in Section 2.2; L is the length of the data series used for grey prediction algorithm.

3. SIMULATION RESULTS

To validate the proposed algorithm, two typical scenarios of maneuvering target tracking are examined: one case corresponds to small maneuvers and the other corresponds to large maneuvers. We compare the performance of the GP-PF with the SPF and the MMPF in terms of tracking accuracy, computational complexity and tracking lost probability. The common parameters used in the two cases are given as follows: sampling interval $T = 0.5$ s; $Q = [4^2, 0; 0, 4^2]$, $R = [20^2, 0; 0, 20^2]$; $\alpha = 0.4$; $L = 10$; The particle number N_p for SPF, MMPF and GP-PF is 1000. We have implemented the algorithms in Matlab 7.1, and simulation results are obtained from 100 independent Monte Carlo runs.

3.1. Case 1: Target Tracking with Small Maneuvers

3.1.1. Target Scenario

The target scenario is generated by

$$x_k = A(T)x_{k-1} + B_u(T)u_k + B(T)w_k \quad (12)$$

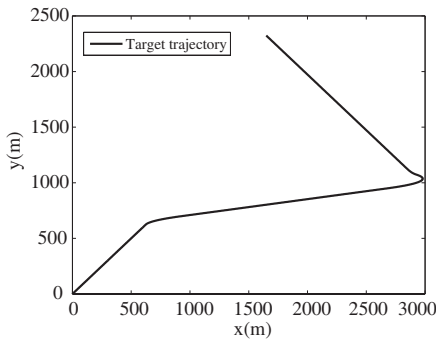


Figure 1. True target trajectory.

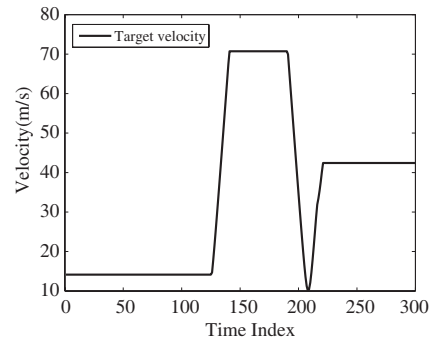


Figure 2. True target velocity.

where $B_u = \begin{pmatrix} T^2/2 & 0 \\ T & 0 \\ 0 & T^2/2 \\ 0 & T \end{pmatrix}$ is the input matrix, $u_k = [u_k^x, u_k^y]'$ is

acceleration input vector [22]. Different u_k in (12) construct different maneuvering models. When using the MMPF, the acceleration u_k is modeled as a first-order Markov chain that takes values from a set of acceleration levels $\{(u_1^x, u_1^y), (u_2^x, u_2^y), \dots, (u_M^x, u_M^y)\}$, with transition probabilities $p_{ij} = P(u_k = m_j | u_{k-1} = m_i), i, j = 1, \dots, M$, where M is the number of the models. Note that (12) will be simplified to the constant velocity model (1), if the term $B_u(T)u_k$ is removed, or equivalently, $u_k = 0$.

The target moves from position (0 m, 0 m) with initial speed (10 m/s, 10 m/s). Table 2 lists the detailed description of the target motion, and the trajectory is shown in Fig. 1. Fig. 2 gives the actual target speed, which shows the maneuver of the target. The particle number for grey prediction is $N_p^{grey} = N_p/10$; The u^x and u^y that construct the model set of MMPF are both from the acceleration set $\{-10, -8, -6, \dots, 6, 8, 10\}$; Transition probabilities $p_{ii} = 0.7$ and $p_{ij} = 0.0025$ for $i \neq j$.

Table 2. Description of target motion.

Time index (0.5 sec)	Target motion
0–125	Constant velocity
126–140	Constant acceleration (8 m/s ² , 0 m/s ²)
141–190	Constant velocity
191–215	Constant acceleration (−8 m/s ² , 0 m/s ²)
216–220	Constant acceleration (0 m/s ² , 8 m/s ²)
221–300	Constant velocity

3.1.2. Tracking Performance Comparison

Figure 3 shows the tracking results by the SPF, the MMPF and the proposed GP-PF. For a more clear view of the differences of the tracking performance by different methods, Fig. 4 shows the root mean squared error (RMSE) of estimated position corresponding to the three filters. It is clear that when the target is during the maneuvering, the SPF can not maintain good tracking accuracy. This is because the

true dynamics of target changes abruptly so the model can no longer represent the target motion well, thus the weights of most particles may become negligible. Under such circumstance, the SPF can not work well. On the contrary, in the proposed GP-PF, because of its combination of model-based and model-free characteristics, even if the particles sampled by the state transition model are useless, those generated by grey prediction also contain information about the target state, which guarantees the tracking accuracy.

When the performance of the proposed GP-PF and the MMPF is compared, from Fig. 4 it can be found that the GP-PF and the MMPF have approximately equal tracking performance, which is also confirmed by the position RMSE comparison listed in Table 3. If detailed comparison of the GP-PF and the MMPF in Fig. 4 is made, it is shown that during maneuvering period, the tracking performance of the MMPF is a little bit better than the proposed GP-PF, and during non-maneuvering period, the performance of GP-PF is a little bit better than the MMPF. This can be explained as follows: When the target is during maneuvering, the sub-models in MMPF can cover the true state of the target better than using GP-PF, which makes the MMPF work better. However, during non-maneuvering, most of models of the MMPF are deviated from the true target dynamics, and the so-called model competition occurs, which degrades the tracking accuracy [35].

Beside the tracking accuracy, the other two important parameters in target tracking are computational complexity and tracking lost probability. For a complete comparison, Table 3 lists the position RMSE (representing tracking accuracy), consumption time (representing computational complexity) and number of tracking lost in 100 Monte Carlo runs (representing tracking lost probability) for

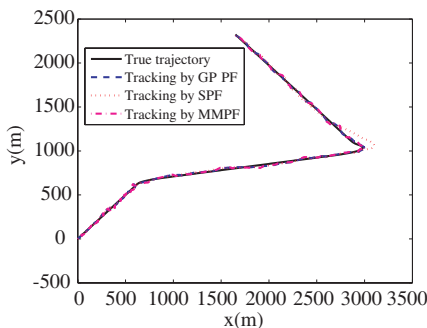


Figure 3. Estimated trajectory by GP-PF, SPF and MMPF.

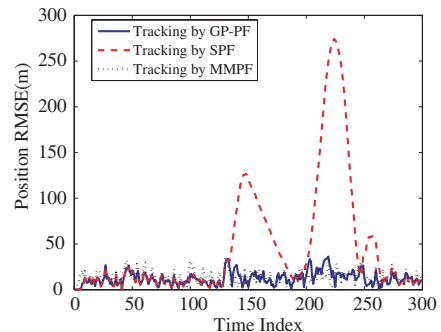


Figure 4. RMSE of position by GP-PF, SPF and MMPF.

the SPF, the MMPF and the GP-PF.

For the comparison of GP-PF and SPF, it is shown in Table 3 that the computing complexity is approximately equal, but the tracking accuracy and the tracking lost performance of the GP-PF is much better than the SPF.

For the comparison of GP-PF and MMPF, it is shown in Table 3 that though the tracking accuracy of MMPF and GP-PF is approximately the same, and both algorithms have no tracking lost, the MMPF consumes much more computation power than the GP-PF. In addition, as described in the former section, the determination of the sub-models of MMPF is difficult in practice. In order to analyze the robustness of the proposed GP-PF to particle number variation, Fig. 5 plots the position RMSE and Fig. 6 plots the number of tracking lost in 100 Monte Carlo runs for different algorithms when the particle number changes from 50 to 2000 and. It is clear that with more particles, the performance of MMPF and GP-PF are nearly the same, and much better than the SPF. However, when the particle number is small, for

Table 3. Tracking performance comparison.

	Position RMSE/m	Consumption Time/s	Number of Tracking Lost
SPF	40.1420	18.5157	6
MMPF	16.2815	31.2451	0
GP-PF	14.6763	18.5462	0

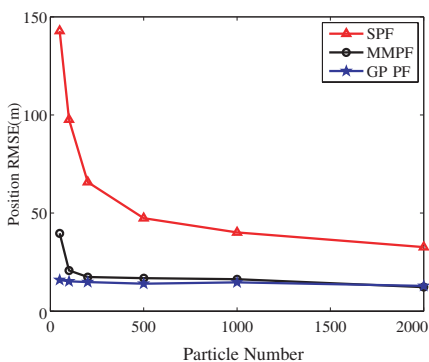


Figure 5. Position RMSE by GP-PF, SPF and MMPF with different particle number.

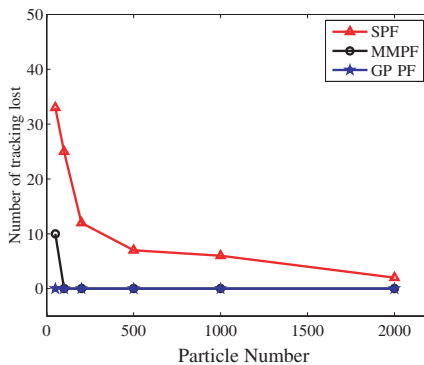


Figure 6. Number of tracking lost by GP-PF, SPF and MMPF with different particle number.

example, only 50 particles are used, the tracking accuracy of MMPF is degraded, and the tracking lost may happen. The reason is that, the MMPF uses many sub-models to cover the target maneuver because of less prior information. When the particle number is small, there may not be enough particles in the models that match the true target dynamics well, which leads to the performance degradation. From Fig. 5 and Fig. 6, the proposed GP-PF is much more robust and can obtain satisfactory results even the total particle number is small.

Table 4 gives the tracking performance of GP-PF with different number of particles used in the grey prediction sampling, when totally 1000 particles are used. It shows that an optimal particle number for grey prediction can be obtained by running simulations. Actually, the choice of N_p^{grey} may be problem dependent: for situations with small maneuvers, small N_p^{grey} is enough, and larger value may be needed when the maneuvers are abrupt and large.

Table 4. Tracking performance of GP-PF with different N_p^{grey} (total particle number is 1000).

N_p^{grey}/N_p	5%	10%	20%	50%	70%	90%
Position RMSE/m	17.0059	14.6763	14.9934	16.1046	25.1046	28.4286
Consumption Time/s	18.97117	18.5462	18.5010	18.3009	18.0909	17.5816

3.2. Case 2: Target Tracking With Large Maneuvers

3.2.1. Target Scenario

In this case, we consider a relatively complicated scenario where the motion pattern of the target changes more largely and the maneuvering period is much longer. The target is modeled by the coordinated turn (CT) model:

$$x_k = F(\theta, T)x_{k-1} + B(T)w_k \quad (13)$$

where $F(\theta, T) = \begin{pmatrix} 1 & \frac{\sin \theta T}{\theta} & 0 & -\frac{1-\cos \theta T}{\theta} \\ 0 & \cos \theta T & 0 & -\sin \theta T \\ 0 & -\frac{1-\cos \theta T}{\theta} & 1 & \frac{\sin \theta T}{\theta} \\ 0 & \sin \theta T & 0 & \cos \theta T \end{pmatrix}$ is the state transition matrix, θ is the turn rate, and the other parameters

are the same as case 1. Different θ in (13) constructs different maneuvering models of MMPF. Different from case 1, in this case, the maneuver information is assumed to be known. The model set is $\{\theta = 0, 6, 9, -7^\circ/\text{s}\}$, transition probabilities $p_{ii} = 0.7$ and $p_{ij} = 0.1$ for $i \neq j$. Based on the analysis of case 1, the particles used in grey prediction sampling is set as $N_p^{grey} = N_p/5$.

Table 5. Description of target motion.

Time index (0.5 sec)	Target motion
0–20	Constant velocity
21–100	Constant turn ($6^\circ/\text{s}$)
101–200	Constant velocity
201–240	Constant turn ($9^\circ/\text{s}$)
241–300	Constant velocity
301–400	Constant turn ($-7^\circ/\text{s}$)
401–440	Constant velocity

The target starts a constant velocity motion from position (1000 m, 1000 m) with initial speed ($u^x = 28 \text{ m/s}$, $u^y = 28 \text{ m/s}$, $\theta = 0^\circ/\text{s}$), Table 5 lists the detailed description of the target motion.

3.2.2. Tracking Performance Comparison

Figure 7 shows the tracking results by the SPF, the MMPF and the GP-PF, and Fig. 8 shows the corresponding position RMSE. It is clear that though the maneuvers are large, good performance can be obtained by the MMPF and GP-PF, while the SPF has much worse tracking performance. The detailed comparisons are listed in the Table 6. Because in this case the maneuvering information is assumed to be known, the sub-modes in MMPF are much less than that in case 1. Consequently, the consumption time by MMPF is less than that in case 1, and the consumption time reduced by GP-PF is not obvious as shown in case 1. However, this kind of prior maneuvering information may be hard to obtain for the MMPF in practice.

Figures 9 and 10 show the position RMSE and number of tracking lost by the three filters with different particle number. From the two figures, the advantage of the proposed GP-PF is more obvious. it is more effective and robust than the SPF and the MMPF.

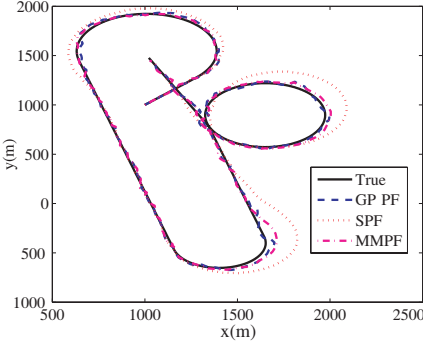


Figure 7. Estimated trajectory by GP-PF, SPF and MMPF.

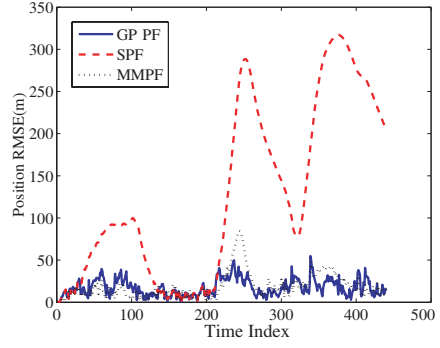


Figure 8. Position RMSE by GP-PF, SPF and MMPF.

Table 6. Tracking performance comparison.

	Position RMSE/m	Consumption Time/s	Number of Tracking Lost
SPF	140.4561	27.5059	12
MMPF	17.0478	30.4121	0
GP-PF	15.6486	27.5814	0

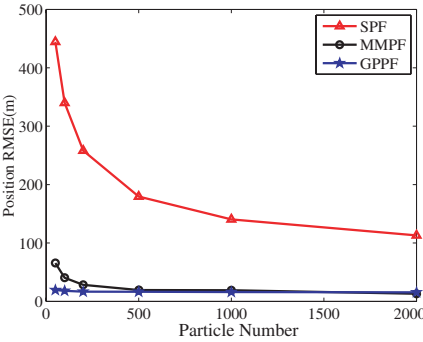


Figure 9. Position RMSE by GP-PF, SPF and MMPF with different particle number.

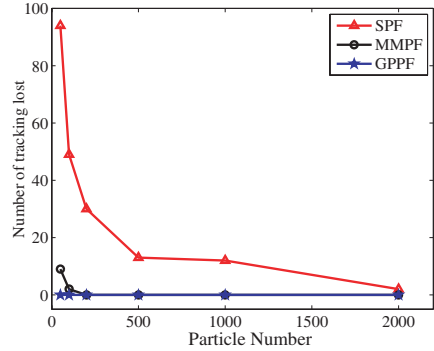


Figure 10. Number of tracking lost by GP-PF, SPF and MMPF with different particle number.

From the above comparisons, one can conclude that the overall performance of the proposed GP-PF is superior to the SPF and the

MMPF. This can be attributed to its model-based and model-free feature.

4. CONCLUSION

A novel GP-PF for maneuvering target tracking has been proposed and its performance is examined. The proposed GP-PF incorporates the grey prediction algorithm into the SPF. The GP-PF algorithm is tested in the context of two typical maneuvering target motion scenarios. The results show that the overall performance of the proposed GP-PF is better than the SPF and the MMPF when the tracking accuracy, computational complexity and tracking lost probability are considered. The performance improvements can be attributed to the model-based and model-free features of the GP-PF.

ACKNOWLEDGMENT

This work was supported by the National Natural Science Foundation of China (No. 60801004 and No. 60604029) and the Natural Science Foundation of Zhejiang Province (No. Y107285 and No. Y106384).

REFERENCES

1. Blackman, S. S., *Multiple Target Tracking with Radar Applications*, Artech House, Norwood, MA, 1986.
2. Bar-Shalom, Y. and T. E. Fortmann, *Tracking and Data Association*, Academic Press, Orlando, 1988.
3. Singh, A. K., P. Kumar, T. Chakravarty, G. Singh, and S. Bhooshan, "A novel digital beamformer with low angle resolution for vehicle tracking radar," *Progress In Electromagnetics Research*, PIER 66, 229–237, 2006.
4. Shi, Z. G., S. Qiao, K. S. Chen, W. Z. Cui, W. Ma, T. Jiang, and L. X. Ran, "Ambiguity functions of direct chaotic radar employing microwave chaotic Colpitts oscillator," *Progress In Electromagnetics Research*, PIER 77, 1–14, 2007.
5. Turkmen, I. and K. Guney, "Tabu search tracker with adaptive neuro-fuzzy inference system for multiple target tracking," *Progress In Electromagnetics Research*, PIER 65, 169–185, 2006.
6. Zang, W., Z. G. Shi, S. C. Du, and K. S. Chen, "Novel roughening method for reentry vehicle tracking using particle filter," *Journal of Electromagnetic Waves and Applications*, Vol. 21, No. 14, 1969–1981, 2007.

7. Bi, S. Z. and X. Y. Ren, "Maneuvering target doppler-bearing tracking with signal time delay using interacting multiple model algorithms," *Progress In Electromagnetics Research*, PIER 87, 15–41, 2008.
8. Tanizaki, H., *Nonlinear Filters: Estimation and Application*, Springer, Berlin, 1996.
9. Bar-Shalom, Y. and X. R. Li, *Multitarget Multisensor Tracking: Principles and Techniques*, YBS Publishing, Storrs, CT, 1995.
10. Chen, J. M., X. Cao, Y. Xiao, and Y. Sun, "Simulated annealing for optimisation with wireless sensor and actuator networks," *Electronics Letters*, Vol. 44, No. 20, 1208–1209, 2008.
11. Gordon, N. J., D. J. Salmond, and A. F. M. Smith, "Novel approach to nonlinear/non-Gaussian Bayesian state estimation," *IEE Proceeding-F*, Vol. 140, No. 2, 107–113, 1993.
12. Doucet, A., N. D. Freitas, and N. Gordon, *Sequential Monte Carlo Methods in Practice*, Springer, New York, 2001.
13. Du, S. C, Z. G. Shi, W. Zang, and K. S. Chen, "Using interacting multiple model particle filter to track airborne targets hidden in blind Doppler," *Journal of Zhejiang University-Science A*, Vol. 8, No. 8, 1277–1282, 2007.
14. Shi, Z. G., S. H. Hong, and K. S. Chen, "Experimental study on tracking the state of analog Chua's circuit with particle filter for chaos synchronization," *Physics Letters A*, Vol. 372, 5575–5580, 2008.
15. Hong, S. H., Z. G. Shi, and K. S. Chen, "Novel roughening algorithm and hardware architecture for bearings-only tracking using particle filter," *Journal of Electromagnetic Waves and Applications*, Vol. 22, 411–422, 2008.
16. Shi, Z. G., S. H. Hong, and K. S. Chen, "Tracking airborne targets hidden in blind doppler using current statistical model particle filter," *Progress In Electromagnetics Research*, PIER 82, 227–240, 2008.
17. Li, Y., Y. J. Gu, Z. G. Shi, and K. S. Chen, "Robust adaptive beamforming based on particle filter with noise unknown," *Progress In Electromagnetics Research*, PIER 90, 151–169, 2009.
18. Wang, X., X. Guan, X. Ma, D. Wang, and Y. Su, "Calculating the poles of complex radar targets," *Journal of Electromagnetic Waves and Applications*, Vol. 20, No. 14, 2065–2076, 2006.
19. Stratakos, Y., G. Geroulis, and N. Uzunoglu, "Analysis of glint phenomenon in a monopulse radar in the presence of skin echo and non-ideal interferometer echo signals," *Journal of Electromagnetic*

- Waves and Applications*, Vol. 19, No. 5, 697–711, 2005.
20. Abdelaziz, A. A., “Improving the performance of an antenna array by using radar absorbing cover,” *Progress In Electromagnetics Research Letters*, Vol. 1, 129–138, 2008.
 21. Chan, Y. K. and S. Y. Lim, “Synthetic aperture radar (SAR) signal generation,” *Progress In Electromagnetics Research B*, Vol. 1, 269–290, 2008.
 22. Li, X. R. and V. P. Jilkov, “Survey of maneuvering target tracking — Part I: Dynamic models,” *IEEE Aerospace and Electronic Systems Magazine*, Vol. 39, No. 4, 1333–1364, 2003.
 23. Blom, H. A. P. and Y. Bar-Shalom, “The interacting multiple model algorithm for systems with Markovian switching coefficients,” *IEEE Transactions on Automatic Control*, Vol. 33, No. 8, 780–783, 1988.
 24. McGinnity, S. and G. W. Irwin, “Multiple model bootstrap filter for maneuvering target tracking,” *IEEE Aerospace and Electronic Systems Magazine*, Vol. 36, No. 3, 1006–1012, 2000.
 25. Boers, Y. and J. N. Driessen, “Interacting multiple model particle filter,” *IEE Proceedings on Radar, Sonar and Navigation*, Vol. 150, No. 5, 344–349, October 2003.
 26. Ristic, B., S. Arulampalam, and N. Gordon, *Beyond the Kalman Filter: Particle Filter for Tracking Applications*, Artech House, Boston, 2004.
 27. Li, X. R. and V. P. Jilkov, “A survey of maneuvering target tracking-Part V: Multiple-model methods,” *IEEE Aerospace and Electronic Systems Magazine*, Vol. 41, No. 4, 1255–1321, 2003.
 28. Arulampalam, S., N. Gordon, M. Orton, and B. Ristic, “A variable structure multiple model particle filter for GMTI tracking,” *Proceedings of 5th International Conference on Information Fusion*, 927–934, Annapolis, USA, July 2002.
 29. Jilkov, V. P., D. S. Angelova, and T. A. Semerdijev, “Design and comparison of mode-set adaptive IMM for maneuvering target tracking,” *IEEE Trans. on Aerosp. Electron. Syst.*, Vol. 35, No. 1, 343–350, 1999.
 30. Luo, R. C., T. M. Chen, and K. L. Su, “Target tracking using hierarchical grey-fuzzy motion decision-making method,” *IEEE Transactions on Systems, Man, and Cybernetics-Part A*, Vol. 31, No. 3, 179–186, 2001.
 31. Luo, R. C. and T. M. Chen, “Target tracking by grey prediction theory and look-ahead fuzzy logic control,” *IEEE International Conference on Robotics and Automation*, 1176–1181, Detroit,

- America, May 1999.
32. Deng, J. L., "Control problems of grey system," *Systems and Control Letters*, Vol. 5, 288–294, 1982.
 33. Wong, C. C., B. C. Lin, and C. T. Cheng, "Fuzzy tracking method with a switching grey prediction for mobile robot," *IEEE International Conference on Fuzzy Systems*, 103–106, Melbourne, Australia, December 2001.
 34. Arulampalam, M. S., S. Maskell, N. Gordon, and T. Clapp, "A tutorial on particle filters for online nonlinear/non-Gaussian Bayesian tracking," *IEEE Transaction on Signal Processing*, Vol. 50, No. 2, 174–188, 2002.
 35. Li, X. R. and Y. Bar-Shalom, "Multiple-model estimation with variable structure," *IEEE Transactions on Automatic Control*, Vol. 41, No. 4, 478–493, 1996.